ACS APPLIED MATERIALS & INTERFACES

Research Article

Cite This: ACS Appl. Mater. Interfaces 2019, 11, 10351−10355

www.acsami.org

Resonant and Selective Excitation of Photocatalytically Active Defect Sites in TiO_2

Bingya Hou,[†] Lang Shen,[‡] Haotian Shi,[§] Jihan Chen,[†] Bofan Zhao,[†] Kun Li,[⊥] Yi Wang,[§] Guozhen Shen,[#] Mai-Anh Ha,[¶] Fanxi Liu,[▽] Anastassia N. Alexandrova,[¶,○] Wei Hsuan Hung,[♦] Jahan Dawlaty,[§] Phillip Christopher,[⊥] and Stephen B. Cronin*[,†,§,∥]

[†]Ming Hsieh Department of Electrical Engineering, [‡]Mork Family Department of Chemical Engineering and Materials Science, [§]Department of Chemistry, and [∥]Department of Physics and Astronomy, University of Southern California, Los Angeles, California 90089, United States

[⊥]Department of Chemical Engineering, University of California, Santa Barbara, Santa Barbara, California 93106-5080, United States

[#]State Key Laboratory for Superlattices and Microstructures, Institute of Semiconductors, Chinese Academy of Science, Beijing 100083, P. R. China

[¶]Department of Chemistry and Biochemistry, California NanoSystems Institute, University of California, Los Angeles, Los Angeles, California 90025, United States

[▽]Collaborative Innovation Center for Information Technology in Biological and Medical Physics, and College of Science, Zhejiang University of Technology, Hangzhou 310023, P. R. China

[○]Materials Sciences Division, Lawrence National Laboratory, Berkeley, California 94720, United States

[♦]Department of Materials Science and Engineering, Feng Chia University, Taichung 407, 40724, Taiwan

Supporting Information

ABSTRACT: It has been known for several decades that defects are largely responsible for the catalytically active sites on metal and semiconductor surfaces. However, it is difficult to directly probe these active sites because the defects associated with them are often relatively rare with respect to the stoichiometric crystalline surface. In the work presented here, we demonstrate a method to selectively probe defect-mediated photocatalysis through differential alternating current (ac) photocurrent (PC) measurements. In this approach, electrons are photoexcited from the valence band to a relatively narrow distribution of subband gap states in TiO_2 and then subsequently to the ions in solution. Because of their limited number, these defect states fill up quickly, resulting in Pauli blocking, and are thereby undetectable under direct current or continuous wave excitation. In the method demonstrated here, the incident light is modulated with an optical chopper, whereas the PC is measured with a lock-in amplifier. Thin (5 nm) films of TiO_2 deposited by atomic layer deposition on various metal films, including Au, Cu, and Al, exhibit the same wavelength-dependent PC spectra, with a broad peak centered around 2.0 eV corresponding to the band-to-defect transition associated with the hydrogen evolution reaction (HER). While the UV−vis absorption spectra of these films show no features at 2.0 eV, photoluminescence (PL) spectra of these photoelectrodes show a similar wavelength dependence with a peak of around 2.0 eV, corresponding to the subband gap emission associated with these defect sites. As a control, alumina (Al_2O_3) films exhibit no PL or PC over the visible wavelength range. The ac PC plotted as a function of electrode potential shows a peak of around −0.4 to −0.1 V versus normal hydrogen electrode, as the monoenergetic defect states are tuned through a resonance with the HER potential. This approach enables the direct photoexcitation of catalytically active defect sites to be studied selectively without the interference of the continuum interband transitions or the effects of Pauli blocking, which is limited by the slow turnover time of the catalytically active sites, typically on the order of 1 μs. We believe that this general approach provides an important new way to study the role of defects in catalysis in an area where selective spectroscopic studies of these are few.

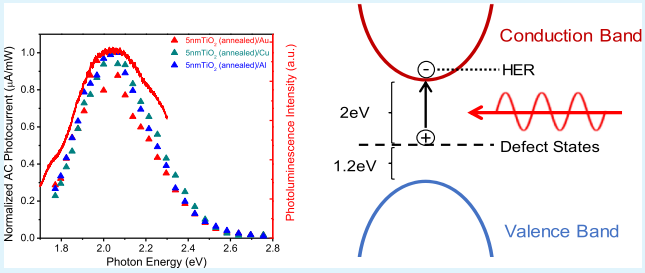

KEYWORDS: *titania, titanium dioxide, resonate, photocatalysis, active site, catalysis*

Defects in TiO_2 have been studied extensively, providing an important mechanism in photocatalytic energy conversion. In particular, oxygen vacancies (i.e., Ti^{3+} states) have been linked to catalytically active sites, particularly in the

Received: July 25, 2018
Accepted: February 15, 2019
Published: February 15, 2019

DOI: 10.1021/acsami.8b12621
ACS Appl. Mater. Interfaces 2019, 11, 10351−10355

water splitting and CO_2 reduction reaction systems.[1] TiO_2 films deposited by atomic layer deposition (ALD) are also known to have a high concentration of defects and, hence, show enhanced water splitting and CO_2 reduction efficiencies.[2−5] Qiu et al. have quantified these O vacancies (i.e., Ti^{3+} states) in ALD-deposited TiO_2 films using X-ray photoelectron spectroscopy (XPS), and they have correlated these vacancies with the photocatalytic activity of TiO_2 films for both water splitting and CO_2 reduction reactions.[2,4] Density functional theory (DFT) calculations performed by Alexandrova's group have provided an atomistic picture of this enhancement mechanism, which show that both H_2O and CO_2 molecules bind stably to these nonstoichiometric Ti^{3+} states.[3,6] Furthermore, when they allow their calculations to relax to their quantum mechanical ground state, they observe a spontaneous transfer of one electron creating CO_2^-. In these DFT calculations, this CO_2^- species is bent and represents a high barrier intermediate species in this difficult reaction system.

In addition to oxygen vacancies, nitrogen defects can be created in TiO_2 by annealing in NH_3 gas, resulting in substantial subband gap absorption.[7−9] This is a well-studied system in which the N-defect concentration can be controlled up to several percent by varying the annealing temperature. Extensive surface science studies of N-doping have been performed in the research groups of Rodriguez[10] and Yates.[11−13] Doping of metal oxides by ion implantation, followed by calcination in oxygen, has also been studied extensively as a means of dramatically increasing in the photocatalytic activity in the visible wavelength range.[14−23] Among the elements studied, V, Cr, Mn, Fe, and Ni were found to increase the photocatalytic activity of TiO_2 in the visible range substantially.[24]

In the work presented here, an alternating current (ac) lock-in measurement technique is employed to study photocatalysis, revealing the behavior of subband gap states that are resonant in both wavelength and electrode potential and give rise to a substantial increase in photocurrent (PC) in the hydrogen evolution reaction (HER) process. In order to further characterize these subband gap states, we collect photoluminescence (PL) spectra, which provide an independent measure of the energetics of these important subband gap states. UV−vis spectra are also obtained in order to provide a complete picture of the band edge and subband gap absorption in the TiO_2 thin film with and without annealing.

Photoelectrodes were fabricated by depositing 100 nm thick films of Au, Cu, and Al on glass substrates using electron beam deposition. A 5 nm TiO_2 film was then deposited by ALD at 250 °C using tetrakis(dimethylamido)titanium as the Ti source and water vapor as the O source. The base flow rate during deposition was 20 sccm. The TiO_2 thickness was established by ellipsometry for a 5 nm film, which corresponds to 100 ALD cycles. The TiO_2/Au films were annealed in a quartz tube furnace at 450 °C for 30 min while O_2 gas was flowing. The TiO_2/Cu and TiO_2/Al films were annealed in a quartz tube furnace at 450 °C for 30 min while argon gas was flowing. UV−vis absorption spectra of a 10 nm thick TiO_2 film taken before and after annealing are plotted in Figure S1 of the Supporting Information. Figure 1a shows an illustration of the sample geometry, in which an insulated copper wire was attached to the TiO_2/metal electrode using silver paint, and the whole sample, excluding the top surface, was encased in epoxy to insulate it from the electrolytic solution. Photoelectrochemical measurements were performed using a three-terminal potentiostat (Gamry, Inc.), as illustrated in Figure 1b. For the HER, a Ag/AgCl reference electrode was used and a Pt wire was used as the counter electrode. The electrodes were immersed in a pH = 7, Na_2SO_4 solution. We used an ac lock-in technique, which enables us to detect the relatively small PCs (μA) produced by just 5 nm of a wide band gap semiconductor material. In order to vary the wavelength of the incident light, a 1000 W xenon lamp was used in conjunction with a monochromator to produce monochromatic light throughout the visible wavelength range. The power reaching the sample surface was 2−3 mW. Here, the light was filling the entire sample area. The incident light was chopped at frequency $\omega_{chopper}$, which was 200 Hz in our case. The chopper controller (Stanford Research Systems, Inc., model SR540) was connected to the "REF IN" terminal of the lock-in amplifier (Standard Research Systems, model SRS830 DSP), in order to synchronize the lock-in amplifier with the light modulation. The ac voltage signal from the auxiliary current monitor terminal of the potentiostat was used as the input signal of the lock-in amplifier in order to collect the ac PC generated by the TiO_2/metal films.

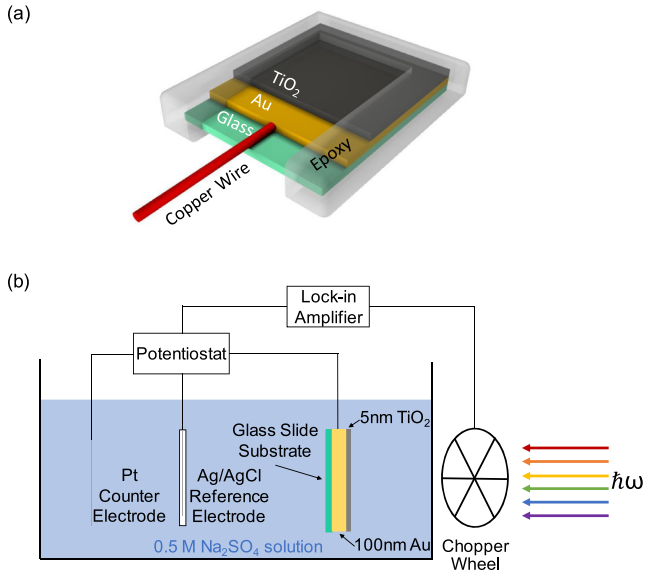

Figure 1. (a) Diagram illustrating the sample configuration. (b) Schematic diagram of the three-terminal photoelectrochemical setup with the modulated light and ac lock-in amplifier.

Figure 2 shows the ac and direct current (dc) PCs plotted as a function of the reference potential for the HER for 5 nm TiO_2 deposited on Au and Cu. Here, we observe a peak in the ac PC around −0.13 V versus normal hydrogen electrode (NHE) corresponding to the conditions under which we tune the potential of the charge associated with the resonantly excited defect states through the redox potential of the HER half-reaction. This is considerably shifted from the dc onset potential of −0.3 V versus NHE. For the TiO_2/Cu electrode, the peak in ac PC is observed at −0.4 V versus NHE, which is also substantially shifted with respect to the dc onset potential of −0.6 V versus NHE.

Figure S4 shows the light intensity dependence of the ac PC from a TiO_2/Au sample obtained for both reduction and oxidation reactions under 532 nm illumination. Here, we observe a linear response to the light intensity, as expected.

DOI: 10.1021/acsami.8b12621
ACS Appl. Mater. Interfaces 2019, 11, 10351−10355

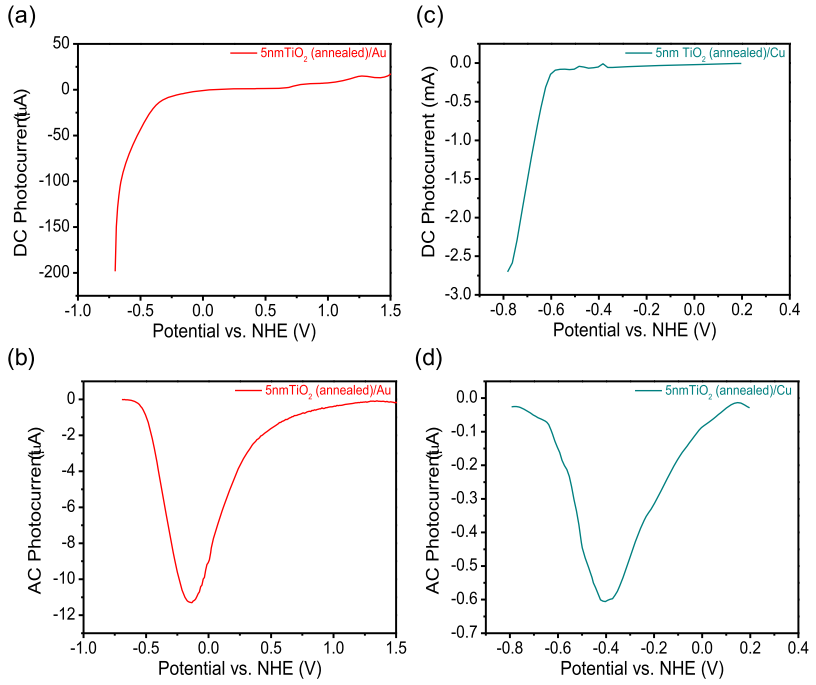

Figure 2. dc (a,c) and ac (b,d) PC plotted as a function of the reference potential for the HER for (a,b) 5 nm annealed TiO_2 deposited on Au under 532 nm illumination and (c,d) 5 nm annealed TiO_2 deposited on Cu under 532 nm illumination.

This result indicates that we are successfully converting photons to hot carriers under optical excitation.[25]

Figure 3a shows the normalized ac PC spectra of 5 nm TiO_2 deposited on Au, Cu, and Al. Here, a clear peak can be seen around 2 eV, which is well below the 3.2 eV band gap of this material. This feature at 2 eV corresponds to the photoexcitation of the subband gap defect states that serve as catalytically active sites for the HER, as illustrated in Figure 3b. Further evidence for this defect state is provided by the PL spectrum, also plotted in Figure 3a, which also exhibits a peak centered around 2.0 eV. Interestingly, no such feature can be seen in the UV−vis absorption spectra at 2.0 eV. Figure S1 of the Supporting Information shows the UV−vis absorption spectra of both annealed and unannealed TiO_2 films. Here, both spectra show moderate subband gap absorption that is monotonically decreasing with wavelength. However, no specific feature is present in these UV−vis spectra at 2.0 eV. This indicates that although there are likely many different types of defect states throughout the band gap, there is a specific defect located at 1.2 eV above the valence band edge that is catalytically active for the HER.

Ultraviolet photoemission spectroscopy (UPS) is a common tool to study conduction and valence band structure of materials.[26,27] The valence band spectrum of an oxygen-annealed 5 nm TiO_2 film was obtained by UPS at 21.2 eV photon energy. The linear plot, Figure 4a, shows the position of valence band edge. The valence band edge is 3.2 eV below the Fermi energy, which is pinned at the conduction band edge. After annealing, a peak at approximately 2 eV below the conduction band edge was observed in the log plot, as shown in Figure 4b, which agrees with the peak position of PC spectra.

Figure S3 shows an XPS spectrum of a 5 nm TiO_2 film deposited on a Au film by ALD. In addition to the main Ti^{4+} peaks, which correspond to stoichiometric TiO_2, we observe a small shoulder peak corresponding to Ti^{3+} states (i.e., oxygen vacancies), as reported previously by Qiu et al.[28]

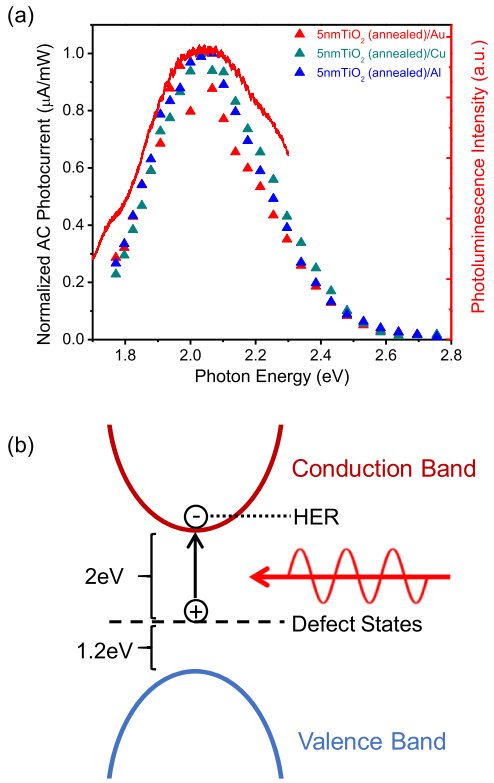

Figure 3. (a) Normalized ac PC spectra of 5 nm TiO_2 deposited on Au, Cu, and Al films and corresponding PL spectrum of 5 nm thick annealed TiO_2 deposited on a Au film. (b) Energy band diagram of the photoexcitation mechanism of defect-mediated photocatalysis.

High-resolution cross-sectional transmission electron microscopy (TEM) images were taken of 5 and 25 nm thick TiO_2

DOI: 10.1021/acsami.8b12621
ACS Appl. Mater. Interfaces 2019, 11, 10351−10355

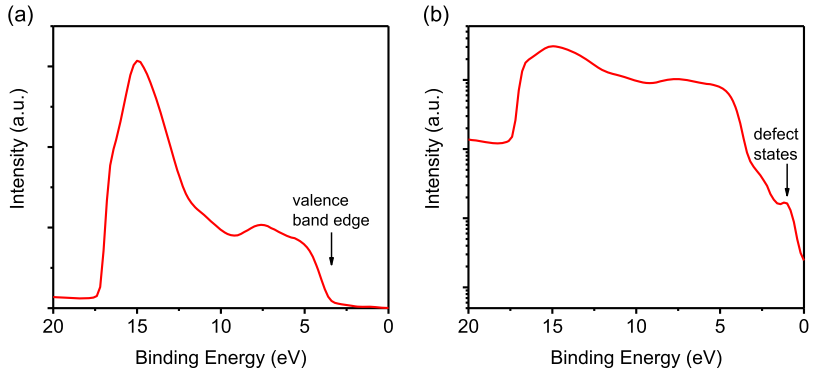

Figure 4. Valence band spectra of a 5 nm TiO_2 film obtained by UPS at 21.2 eV photon energy plotted on (a) linear and (b) log scales.

films deposited on Au films. Figure S2c shows an amorphous TiO_2 material, as expected. This material is nonstoichiometric and contains a high density of oxygen vacancies, as evidenced by the UPS and XPS spectra described above. In contrast, Figure S2d shows a crystalline material. Qiu et al. have also demonstrated that above 10 nm, TiO_2 films become crystalline.[29] These thicker TiO_2 films are crystalline and have poor charge-transfer characteristics because of their insulating nature. Thus, we are more interested in thin and amorphous TiO_2 films.

Plane-wave DFT calculations were performed on defective (101) anatase in order to extract formation energies and spectral analyses of oxygen vacancies. A single oxygen vacancy results in the presence of two excess electrons that may localize on neighboring Ti atoms. Experimentally, spectral signatures were found to be ∼2 eV from the Fermi energy. Because of the overdelocalization of electrons in DFT, we introduced a strong Hubbard *U* parameter of 4.0 eV into our calculations in order to recover a theoretical band gap of ∼2.2 eV. Utilizing Bader charge analysis, we were able to determine the localization of electrons on surface Ti sites. For surface oxygen vacancies V_{O1} and V_{O2}, electrons localized on neighboring Ti atoms ∼1.9 Å from the vacancy site. For surface oxygen vacancy V_{O3}, the two electrons localized on Ti atoms farther away from the vacancy site, one on a Ti atom ∼1.9 Å and the other on a Ti atom ∼3.7 Å from the vacancy site. The ramifications of this may be found in the theoretical density of states shown in Figure S7b. In comparison to V_{O1-O2}, V_{O3}'s spectral signatures of the localized electrons are shifted farther away from the Fermi energy. We hypothesize that at the deeper oxygen vacancy sites, the spectral signatures of the localized electrons also shift farther away from the Fermi energy. However, the small theoretical band gap of ∼2.2 eV may obscure these spectral signatures, and so, we focus only on V_{O1-O3}. On the basis of these DFT calculations, it seems that the specific catalytically active defect sites that we observe in our photoelectrochemical measurements actually correspond to subsurface defects. While these results provide qualitative agreement with our experimental results (i.e., subband gap states giving rise to visible light absorption), it is not possible to assign a specific atomic defect to our observation, and it is likely that a large collective ensemble of these defects contributes to the broad spectral distribution observed experimentally.

In our previous work, similar structures consisting of Au films with and without TiO_2 coatings were investigated.[30] For the bare metal electrodes, the mechanism of photocatalysis was attributed to hot electrons photoexcited in the metal. The mechanism of PC generation in TiO_2-coated Au electrodes was attributed to hot electron injected by the metal film because of our inability to detect these defect states in the UV−vis absorption process. However, these defect states are slightly elusive because of the Pauli blocking associated with their finite density and slow turnover time, and we now have a better understanding of this system. It should be noted that the photoexcited charge generated at these O-vacancy defect sites is bound to the defect site and is not free to propagate throughout the TiO_2 crystal.

In conclusion, we have demonstrated a method to selectively probe defect-mediated photocatalysis through differential ac PC measurements. Here, we drive the photoexcitation of electrons (or holes) from the valence band to a relatively narrow distribution of subband gap states and then to the ions in solution. Because of their limited number, these defect states fill up quickly, resulting in Pauli blocking, and are undetectable under dc or continuous wave conditions. In the method demonstrated here, the incident light is modulated with an optical chopper and the PC is measured with a lock-in amplifier. Thin (5 nm) films of TiO_2 deposited on different metals (Au, Cu, and Al) using ALD exhibit the same wavelength-dependent PC spectra, with a broad peak centered around 2.0 eV. PL spectra also show a peak at 2.0 eV, corresponding to the subband gap emission associated with these defect sites. In addition, the ac PC shows a peak of around −0.4 to −0.1 V versus NHE, as the monoenergetic defect states are tuned through a resonance with the HER potential. This approach enables the photoexcitation of catalytically active defect sites to be studied selectively without the interference from the continuum of interband transitions or the effects of Pauli blocking, which is quite pronounced because of the slow turnover time (∼1 μs) of the catalytically active sites.

■ ASSOCIATED CONTENT

Supporting Information

The Supporting Information is available free of charge on the ACS Publications website at DOI: 10.1021/acsami.8b12621.

UV−vis absorption spectra, high-resolution TEM images, XPS spectrum, frequency dependence of ac PC, light intensity dependence of ac PC, PL spectra, transient absorption spectra, DFT calculation, and ac PC for 5 and 25 nm annealed TiO_2 (PDF)

■ AUTHOR INFORMATION

Corresponding Author

*E-mail: scronin@usc.edu.

DOI: 10.1021/acsami.8b12621
ACS Appl. Mater. Interfaces 2019, 11, 10351−10355

ORCID

Guozhen Shen: 0000-0002-9755-1647
Anastassia N. Alexandrova: 0000-0002-3003-1911
Wei Hsuan Hung: 0000-0002-9136-8753
Jahan Dawlaty: 0000-0001-5218-847X
Phillip Christopher: 0000-0002-4898-5510
Stephen B. Cronin: 0000-0001-7089-6672

Notes

The authors declare no competing financial interest.

■ ACKNOWLEDGMENTS

This research was supported by Air Force Office of Scientific Research (AFOSR) grant no. FA9550-15-1-0184 (B.H.), National Science Foundation (NSF) award no. CBET-1512505 (L.S. and J.C.), Army Research Office (ARO) award no. W911NF-14-1-0228 (H.S.), U.S. Department of Energy, Office of Science, Office of Basic Energy Sciences, award no. DE-SC0019322 (B.Z.), National Science Foundation (NSF) CAREER award no. CHE-1351968 (A.N.A.) and Army Research Office (ARO) grant no. W911NF-17-1-0340 (P.C.).

■ REFERENCES

(1) Lu, G.; Linsebigler, A.; Yates, J. T., Jr. Ti^{3+} Defect Sites on TiO_2(110): Production and Chemical Detection of Active Sites. *J. Phys. Chem. C* **1994**, *98*, 11733−11738.

(2) Qiu, J.; Zeng, G.; Ge, M.; Arab, S.; Mecklenburg, M.; Hou, B.; Shen, C.; Benderskii, A. V.; Cronin, S. B. Correlation of Ti^{3+} states with Photocatalytic Enhancement in TiO_2-passivated p-GaAs. *J. Catal.* **2016**, *337*, 133−137.

(3) Qiu, J.; Zeng, G.; Ha, M.-A.; Hou, B.; Mecklenburg, M.; Shi, H.; Alexandrova, A. N.; Cronin, S. B. Microscopic Study of Atomic Layer Deposition of TiO_2 on GaAs and Its Photocatalytic Application. *Chem. Mater.* **2015**, *27*, 7977−7981.

(4) Zeng, G.; Qiu, J.; Hou, B.; Shi, H.; Lin, Y.; Hettick, M.; Javey, A.; Cronin, S. B. Enhanced Photocatalytic Reduction of CO_2 to CO through TiO_2 Passivation of InP in Ionic Liquids. *Chem.—Eur. J.* **2015**, *21*, 13502.

(5) Zeng, G.; Qiu, J.; Li, Z.; Pavaskar, P.; Cronin, S. B. CO_2 Reduction to Methanol on TiO_2-Passivated GaP Photocatalysts. *ACS Catal.* **2014**, *4*, 3512.

(6) Qiu, J.; Zeng, G.; Ha, M.-A.; Ge, M.; Lin, Y.; Hettick, M.; Hou, B.; Alexandrova, A. N.; Javey, A.; Cronin, S. B. Artificial Photosynthesis on TiO_2-Passivated InP Nanopillars. *Nano Lett.* **2015**, *15*, 6177−6181.

(7) Linic, S.; Christopher, P.; Ingram, D. B. Plasmonic-Metal Nanostructures for Efficient Conversion of Solar to Chemical Energy. *Nat. Mater.* **2011**, *10*, 911−921.

(8) Irie, H.; Watanabe, Y.; Hashimoto, K. Nitrogen-Concentration Dependence on Photocatalytic Activity of $TiO_{2-x}N_x$ Powders. *J. Phys. Chem. B* **2003**, *107*, 5483−5486.

(9) Asahi, R.; Morikawa, T.; Ohwaki, T.; Aoki, K.; Taga, Y. Visible-Light Photocatalysis in Nitrogen-Doped Titanium Oxides. *Science* **2001**, *293*, 269−271.

(10) Nambu, A.; Graciani, J.; Rodriguez, J. A.; Wu, Q.; Fujita, E.; Sanz, J. F. N Doping of TiO_2(110): Photoemission and Density-Functional Studies. *J. Chem. Phys.* **2006**, *125*, 094706.

(11) Thompson, T. L.; Yates, J. T. Control of a Surface Photochemical Process by Fractal Electron Transport across the Surface: O^{-2} Photodesorption from TiO_2(110). *J. Phys. Chem. B* **2006**, *110*, 7431−7435.

(12) Diwald, O.; Thompson, T. L.; Zubkov, T.; Walck, S. D.; Yates, J. T.; Yates, J. T. Photochemical Activity of Nitrogen-Doped Rutile TiO_2(111) in Visible Light. *J. Phys. Chem. B* **2004**, *108*, 6004−6008.

(13) Diwald, O.; Thompson, T. L.; Goralski, E. G.; Walck, S. D.; Yates, J. T. The effect of nitrogen ion implantation on the photoactivity of TiO_2 rutile single crystals. *J. Phys. Chem. B* **2004**, *108*, 52−57.

(14) Anpo, M.; Dohshi, S.; Kitano, M.; Hu, Y.; Takeuchi, M.; Matsuoka, M. The Preparation and Characterization of Highly Efficient Titanium Oxide-Based Photofunctional Materials. *Annu. Rev. Mater. Res.* **2005**, *35*, 1−27.

(15) Yamashita, H.; Harada, M.; Misaka, J.; Takeuchi, M.; Neppolian, B.; Anpo, M. Photocatalytic Degradation of Organic Compounds Diluted in Water Using Visible Light-Responsive Metal Ion-Implanted TiO_2 Catalysts: Fe Ion-Implanted TiO_2. *Catal. Today* **2003**, *84*, 191−196.

(16) Yamashita, H.; Harada, M.; Misaka, J.; Takeuchi, M.; Ikeue, K.; Anpo, M. Degradation of Propanol Diluted in Water Under Visible Light Irradiation Using Metal Ion-Implanted Titanium Dioxide Photocatalysts. *J. Photochem. Photobiol., A* **2002**, *148*, 257−261.

(17) Takeuchi, M.; Yamashita, H.; Matsuoka, M.; Anpo, M.; Hirao, T.; Itoh, N.; Iwamoto, N. Photocatalytic Decomposition of NO on Titanium Oxide Thin Film Photocatalysts Prepared by an Ionized Cluster Beam Technique. *Catal. Lett.* **2000**, *66*, 185−187.

(18) Yamashita, H.; Harada, M.; Misaka, J.; Takeuchi, M.; Ichihashi, Y.; Goto, F.; Ishida, M.; Sasaki, T.; Anpo, M. Application of Ion Beam Techniques for Preparation of Metal Ion-Implanted TiO_2 Thin Film Photocatalyst Available Under Visible Light Irradiation: Metal Ion-Implantation and Ionized Cluster Beam Method. *J. Synchrotron Radiat.* **2001**, *8*, 569−571.

(19) Anpo, M. Utilization of TiO_2 Photocatalysts in Green Chemistry. *Pure Appl. Chem.* **2000**, *72*, 1265−1270.

(20) Anpo, M. Use of Visible Light. Second-Generation Titanium Oxide Photocatalysts Prepared by the Application of an Advanced Metal Ion-Implantation Method. *Pure Appl. Chem.* **2000**, *72*, 1787−1792.

(21) Iino, K.; Kitano, M.; Takeuchi, M.; Matsuoka, M.; Anpo, M. Design and Development of Second-Generation Titanium Oxide Photocatalyst Materials Operating Under Visible Light Irradiation by Applying Advanced Ion-Engineering Techniques. *Curr. Appl. Phys.* **2006**, *6*, 982−986.

(22) Takeuchi, M.; Yamashita, H.; Matsuoka, M.; Anpo, M.; Hirao, T.; Itoh, N.; Iwamoto, N. Photocatalytic Decomposition of NO Under Visible Light Irradiation on the Cr-Ion-Implanted TiO_2 Thin Film Photocatalyst. *Catal. Lett.* **2000**, *67*, 135−137.

(23) Anpo, M.; Che, M. Applications of Photoluminescence Techniques to the Characterization of Solid Surfaces in Relation to Adsorption, Catalysis, and Photocatalysis. *Adv. Catal.* **2000**, *44*, 119−257.

(24) Choi, W.; Termin, A.; Hoffmann, M. R. The Role of Metal-Ion Dopants in Quantum-Sized TiO_2 - Correlation between Photoreactivity and Charge-Carrier Recombination Dynamics. *J. Phys. Chem.* **1994**, *98*, 13669−13679.

(25) Mukherjee, S.; Zhou, L.; Goodman, A. M.; Large, N.; Ayala-Orozco, C.; Zhang, Y.; Nordlander, P.; Halas, N. J. Hot-Electron-Induced Dissociation of H_2 on Gold Nanoparticles Supported on SiO_2. *J. Am. Chem. Soc.* **2014**, *136*, 64−67.

(26) Fleming, L.; Fulton, C. C.; Lucovsky, G.; Rowe, J. E.; Ulrich, M. D.; Lüning, J. Local Bonding Analysis of the Valence and Conduction Band Features of TiO_2. *J. Appl. Phys.* **2007**, *102*, 033707.

(27) Tao, J.; Luttrell, T.; Batzill, M. A Two-Dimensional Phase of TiO_2 with a Reduced Bandgap. *Nat. Chem.* **2011**, *3*, 296.

(28) Qiu, J.; Zeng, G.; Ge, M.; Arab, S.; Mecklenburg, M.; Hou, B.; Shen, C.; Benderskii, A. V.; Cronin, S. B. Correlation of Ti^{3+} States with Photocatalytic Enhancement in TiO_2-Passivated p-GaAs. *J. Catal.* **2016**, *337*, 133−137.

(29) Qiu, J.; Zeng, G.; Ha, M.-A.; Hou, B.; Mecklenburg, M.; Shi, H.; Alexandrova, A. N.; Cronin, S. B. Microscopic Study of Atomic Layer Deposition of TiO_2 on GaAs and Its Photocatalytic Application. *Chem. Mater.* **2015**, *27*, 7977−7981.

(30) Hou, B.; Shen, L.; Shi, H.; Kapadia, R.; Cronin, S. B. Hot Electron-Driven Photocatalytic Water Splitting. *Phys. Chem. Chem. Phys.* **2017**, *19*, 2877−2881.

DOI: 10.1021/acsami.8b12621
ACS Appl. Mater. Interfaces 2019, 11, 10351−10355